CHEMISTRY
A EUROPEAN JOURNAL

ChemPubSoc Europe

DOI: 10.1002/chem.201103954

Localization/Delocalization of Charges in Bay-Linked Perylene Bisimides

Wei Jiang,[a] Chengyi Xiao,[a] Linxiao Hao,[a] Zhaohui Wang,*[a] Harald Ceymann,[b] Christoph Lambert,*[b] Simone Di Motta,[c] and Fabrizia Negri*[c]

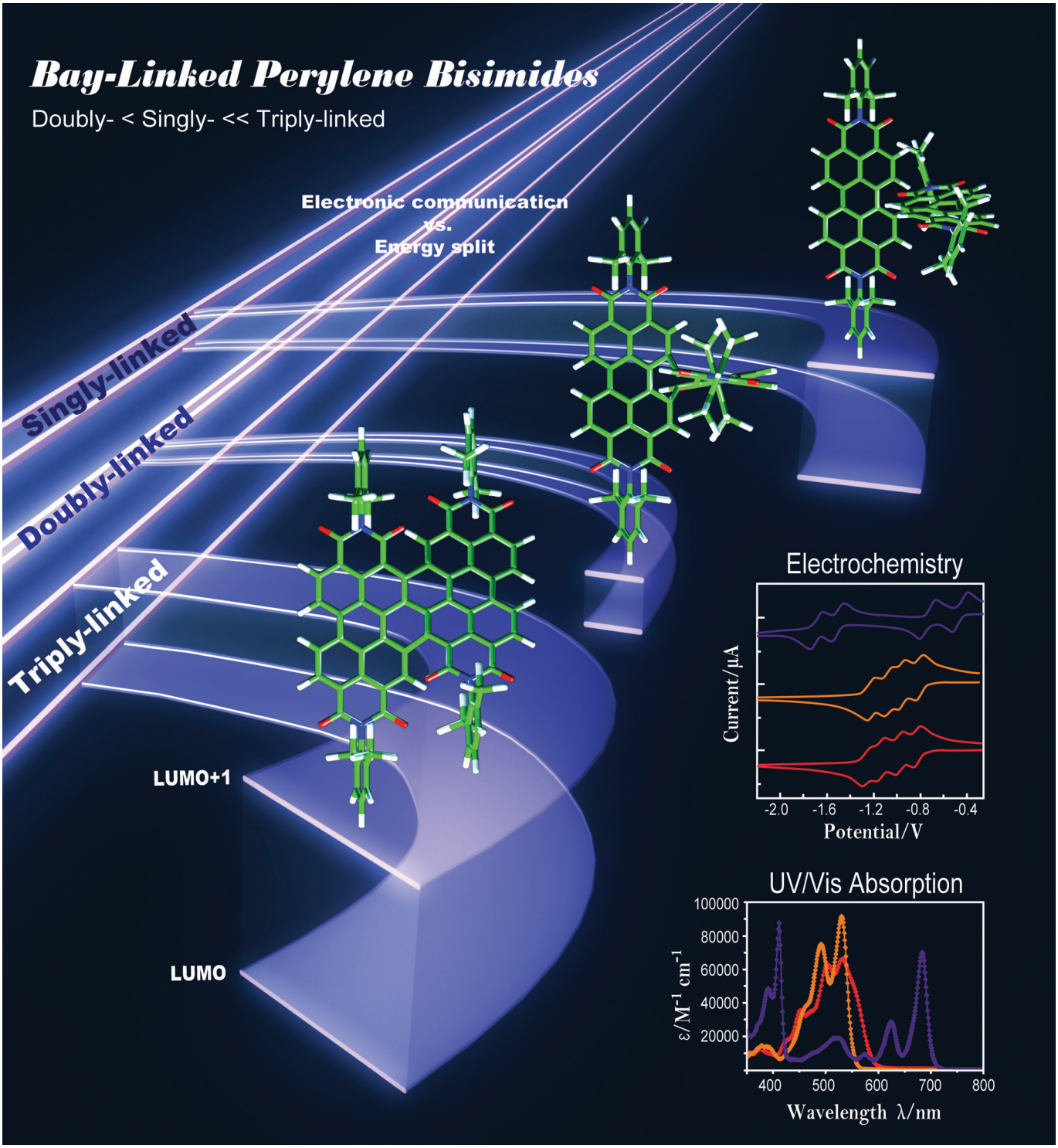

Abstract: The copper-mediated Ullmann coupling of 1,7-dibromoperylene bisimides afforded structurally perfect singly-linked perylene bisimide (PBI) arrays, whilst the homo-coupling of 1,12-dibromoperylene bisimides gave doubly-linked and triply-linked diperylene bisimides. The interactions of three bay-linked diperylene bisimides that differed in their linkage (singly, doubly, and triply) were investigated in their neutral and reduced forms (mono-anion to tetra-anion). UV/Vis absorption and fluorescence spectroscopy revealed different degrees of interaction, which was explained by exciton coupling and conjugation effects. The electrochemical properties and spectroelectrochemistry also showed quite-different degrees of PBI interactions in the reduced mixed-valence species, which was apparent by the observation of CT bands. The interpretation of the experimental findings was supported by spin-restricted and -unrestricted DFT and time-dependent TD-DFT calculations with the long-range-corrected CAM-B3LYP functional. Accordingly, the degree of interaction in both the neutral and reduced forms of the bay-linked PBIs was qualitatively in the order doubly linked < singly linked ≪ triply linked, owing to the different degrees of twisting and flexibility between the two PBIs moieties. Only triply linked diPBI showed completely delocalized wavefunctions over the entire π-system.

Keywords: charge transfer · copper · cross-coupling · perylenes bisimides · Ullmann reaction

Introduction

Functional π-systems with well-defined structures have evoked considerable interest over the past couple of decades in light of their potential applications in molecular electronics.[1] "The larger the π-system, the better the delocalization/stabilization of charge" is a commonly held belief in organic chemistry. Whilst this statement is true for very small π-systems (e.g., naphthalene versus benzene), it is not true for very large systems, in which charge-localization is frequently observed.[2] Herein, we report that, in a series of very large di(perylene bisimides) (which have four times more π-carbon atoms than naphthalene), triple linkage leads to charge-delocalization whereas double- or single linkage leads to charge-localization.

Typically, the reason for charge-localization is a competition between the gain in resonance energy by charge-delocalization and the gain in energy by structural distortion.[3] To these effects, the additional gain in energy through solvent interactions and ion-pairing with counterions favors charge-localization. The structural distortion that goes along with charge-localization is often named "Peierls′ distortion", in particular in the case of solid-state materials.[4] In organic and inorganic molecular chemistry, the localization versus delocalization of charge, along with possible charge-transfer phenomena, is frequently explained by the concept of mixed-valence (MV) chemistry.[2b] In the simplest case, a two-state model is used to outline the electronic situation: two redox centers in different redox states are connected within one molecular unit. The two diabatic, formally non-interacting states, in which a charge is localized on either of the two redox centers, may then be coupled through an electronic coupling interaction to yield two adiabatic states (ground and excited) that represent the physically observable states. In the adiabatic ground state, the charge may then be localized on one or the other redox center (a so-called Robin–Day class II situation)[5] or be delocalized between both redox centers (a Robin–Day class III situation). For Robin–Day class II systems, the rate of electron transfer between the two redox centers is determined by the electronic coupling (V) and the barrier (and thus the shape of the ground-state potential) between the state minima along the reaction coordinate.[6] According to Marcus, the barrier is associated with a fraction (approximately one quarter) of the reorganization energy (λ).[7] The latter energy refers to the structural changes that are needed for making charge-transfer possible. By using these terms and the harmonic approximation for the diabatic states, resonance energy is given by V^2/λ, which leads to delocalization, the larger V and the smaller λ is. Thus, if complete delocalization of a charge is wanted, one aims at increasing V and decreasing λ, which is particularly difficult for large π-systems; as for class II systems, V usually gets smaller and λ increases the larger the π-system is.[8] Both trends could be counteracted by forming stiff π-systems, which led us to consider perylene bisimides (PBIs). We also note that PBIs have hitherto not been employed as redox centers in a mixed-valence-chemistry context.

[a] Dr. W. Jiang, C. Xiao, L. Hao, Prof. Z. Wang
Beijing National Laboratory for Molecular Sciences
Institute of Chemistry, Chinese Academy of Sciences
Beijing 100190 (P.R. China)
Fax: (+86) 10-62650811
E-mail: wangzhaohui@iccas.ac.cn

[b] H. Ceymann, Prof. C. Lambert
Institut für Organische Chemie, Universität Würzburg
Wilhelm Conrad Röntgen Research Center for
Complex Material Systems
Am Hubland, 97074, Würzburg (Germany)
E-mail: christoph.lambert@uni-wuerzburg.de

[c] Dr. S. Di Motta, Prof. F. Negri
Dipartimento di Chimica "G. Ciamician"
Università di Bologna, Via F. Selmi, 2
40126 Bologna, Italy and INSTM, UdR Bologna (Italy)
E-mail: fabrizia.negri@unibo.it

Supporting information for this article is available on the WWW under http://dx.doi.org/10.1002/chem.201103954.

Perylene bisimides (PBIs), which are among the most-intensively investigated chromophores, have been widely used in dye chemistry,[9] supramolecular assemblies,[10] and optoelectronic devices,[11] because they offer a variety of desirable features, such as exceptional electro-optical properties, photochemical stabilities, as well as flexible tunability. PBI derivatives with an extended conjugated core exhibit π-electron delocalization, and thus a low-lying LUMO energy level, which makes them desirable as n-type semiconductors[12] or as near-infrared (NIR) dyes.[13] Recent efforts on the preparation of covalently linked PBI oligomers that are connected by a variety of bridges, such as phenylene, ethynylene, or thieno[3,2−*b*]thiophene units, etc., have focused on the modulation of the structures and properties and the realization of various molecular devices.[14]

Copper-mediated coupling reactions have been widely used in the formation of C–N, C–S, C–O, and C–C bonds.[15] Very recently, some of us synthesized doubly-linked PBI chiral nanoribbons from tetrachloro-PBI by using a simple copper-mediated reaction.[16] Furthermore, a series of fully conjugated triply-linked PBI graphene nanoribbons of up to four units with very broad spectra and strong electron-accepting ability have also been developed by the combination of copper-catalyzed Ullmann-coupling reactions and C–H transformations (Scheme 1).[17] However, these triply-linked oligo-PBIs ($n \geq 1$) had structural isomers, owing to the two possible coupling sites, which led to difficulties in the synthesis and separation of higher homologues. Consequently, to expand the versatility and utility of this synthesis, structurally perfect singly-linked PBI arrays along the bay regions may be a fascinating candidate for exploring new connectivity and for further regiospecifically constructing triply linked PBI oligomers by ring-fusion reactions.

Herein, we report the synthesis of three bay-linked PBIs that differed in their linkage, namely singly, doubly, and triply linked diperylene bisimides (**2**, **9**, and **10**, where $n=0$; Scheme 1). Furthermore, we investigated their static optical properties by UV/Vis absorption and fluorescence spectroscopy as well as their redox properties by cyclic voltammetry. UV/Vis/NIR spectroelectrochemistry was used to characterize their radical anion states. By comparison with DFT-computed electronic couplings, equilibrium structures, and absorption spectra, we will draw conclusions about the electronic structure of this series of diperylene bisimides radical anions.

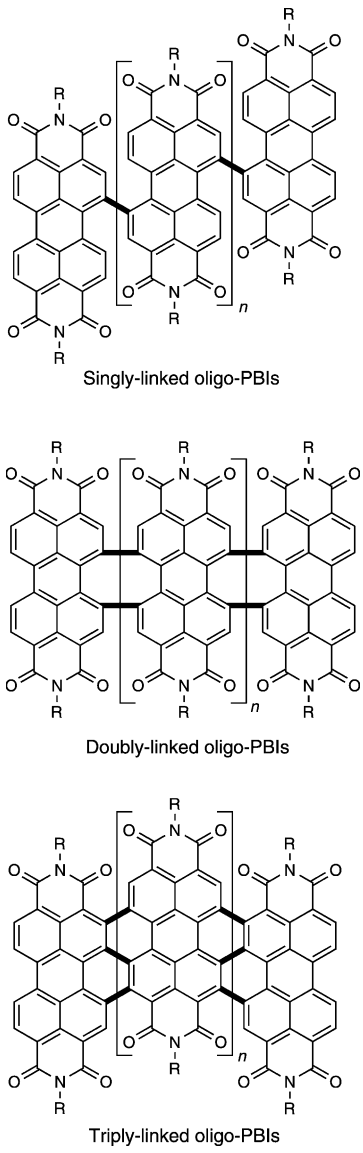

Scheme 1. Three bay-linked PBI-based arrays ($n=0$–x).

Results and Discussion

Synthesis of bay-linked PBIs: Initially, model substrate 1-bromoPBI (**5**) underwent homo-coupling with a stoichiometric amount of nanosized copper powder in dry DMSO at 60 °C to directly afford the corresponding singly-linked diPBI (**2**) in 84.4 % yield (Scheme 2). We envisaged that 1,7-dibromoPBIs could be used as a building block to construct well-defined singly linked PBI-based arrays along the bay regions through copper-mediated Ullmann reactions. As ex-

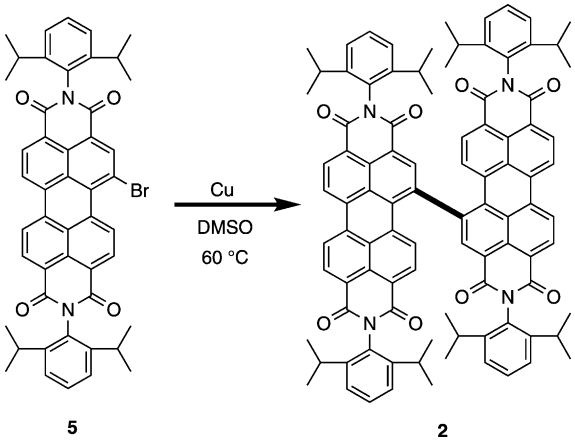

Scheme 2. Synthesis of singly-linked diPBI (**2**) by the Cu-mediated homo-coupling of 1-bromoPBI.

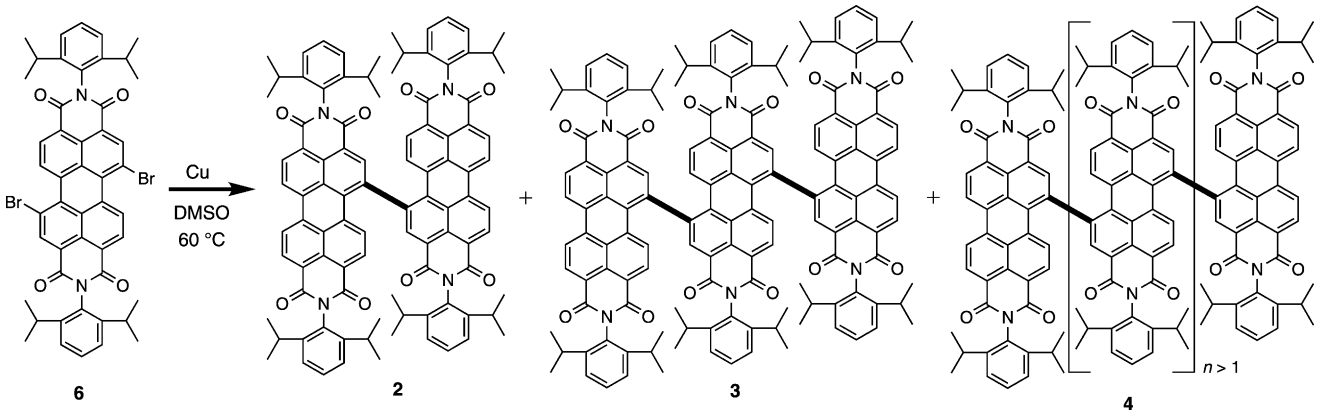

6 2 3 4

Scheme 3. One-pot coupling of 1,7-dibromoPBI for the synthesis of singly-linked PBI arrays.

pected, using 1,7-dibromoPBI (**6**)[18] as the precursor afforded a homologous series of well-defined oligomers, from the dimer up to the octadecamer, as detected by MS (Scheme 3). Separation by column chromatography on silica gel afforded the dimer (**2**) and trimer (**3**) in 14.7% and 9.8% yield, respectively.

The ladder-type arrays should have planar and rigid π-structures that facilitate electron-delocalization and enhance conjugation.[19] As an alternative to 1,7-dibromoPBIs, we anticipated that a 1,12-dibrominated derivative with two bromine atoms in the same bay-region could be used to construct more-rigid, planar π-extended superstructures as a result of the formation of two C–C bonds. Therefore, we examined the homocoupling of 1,12-dibromoPBI (**8**), which was readily prepared from the reaction of 1,6,7,12-tetrabromoPBI (4Br-PBI, **7**), CuI, and L-proline at 60°C in 32.5% yield (65.1% based on the recovered 4Br-PBI). By using the same procedure, doubly linked diPBI (**9**) was obtained as an orange–red solid in 68.7% yield. Surprisingly, a small amount of triply linked diPBI (**10**) was also isolated as a side-product, presumably owing to the efficiency of the Ullmann coupling and C–H transformations (Scheme 4). Our efforts towards the direct coupling of 1,12-dichloroPBI[17e] to produce the desired doubly linked diPBI were unsuccessful, which indicated the low reactivity of 1,12-dichloroPBI.

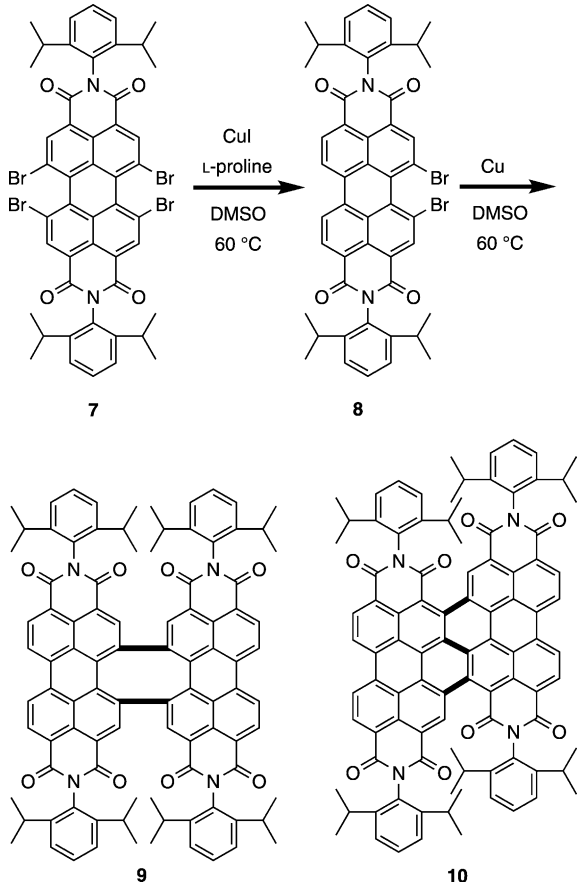

7 8 9 10

Scheme 4. Synthesis of doubly linked (**9**) and triply linked diPBI (**10**).

Optical spectroscopy: The singly linked dimer (**2**) and trimer (**3**) were red–violet solids and were soluble in various organic solvents. The electronic and photophysical properties of the oligomers were studied at room temperature by UV/Vis absorption and emission spectroscopy in $CHCl_3$. Both singly linked dimers (**2** and **3**) showed broader and more-complicated absorption bands than the parent PBI monomer (**1**, Figure 1). Whilst the spectra of compounds **2** and **3** were more alike, they still showed a pronounced red-shift of the onset of absorption (590 nm for compound **2** and 620 nm for compound **3** versus 540 nm for compound **1**). This red-shift and broadening could be interpreted by a combination of effects: first, owing to the flexibility of the singly linked dimers and trimers, a number of slightly different reciprocal orientations of the PBI units were expected, which, in turn, may be associated with different exciton couplings of localized PBI transitions that overall broadened and red-shifted the spectrum.

The significant Stokes shift compared to parent PBI monomer **1** ($\lambda_{em}=534$ nm, $\phi_{fl}=1.0$),[20] and the low fluorescence quantum yield ($\lambda_{em}=605$ nm, $\phi_{fl}=0.15$ for compound **2**; $\lambda_{em}=632$ nm, $\phi_{fl}=0.26$ for compound **3**) were also a consequence of this exciton coupling, if one considered that several twisted conformers contributed to the spectrum. Indeed,

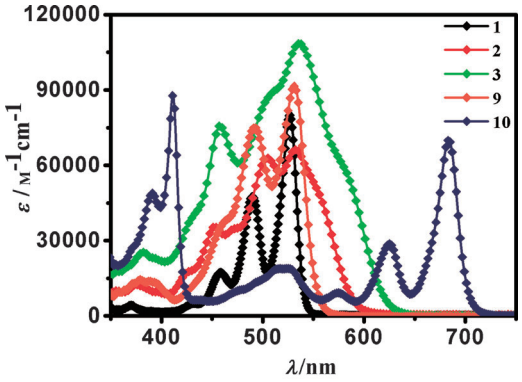

Figure 1. UV/Vis absorption spectra: PBI (**1**, black); singly linked diPBI (**2**, red); triPBI (**3**, green); doubly linked diPBI (**9**, orange); and triply linked diPBI (**10**, violet) in $CHCl_3$.

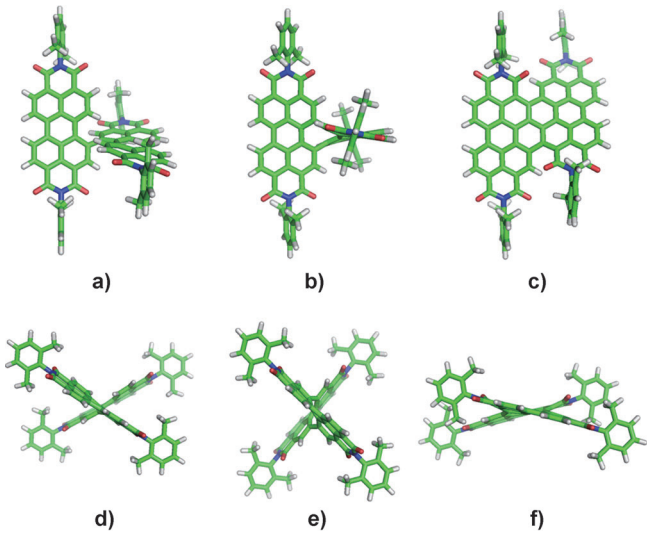

Figure 2. Equilibrium structures (CAM-B3LYP/6-31G*) of the neutral forms of compounds **2** (a, d); **9** (b, e); and **10** (c, f).

the angle between the two PBI π-systems was about 70° for the gas-phase-optimized geometry but, owing to the flexibility of the singly linked derivatives, we expected that a number of different reciprocal orientations of the two PBI units would be populated at room temperature, which followed neither the simple J- or H-type behavior of chromophore aggregates.[21] The magnitude of the exciton coupling was estimated from the energy separation between the two lowest-computed energy transitions of compounds **2** and **9** (see the stick spectra of neutral diPBIs in the Supporting Information, Figures S10 and S11).

In contrast, the absorption spectrum of doubly linked PBI (**9**) was very similar to monomer **1**, just slightly more diffuse with an onset at about 550 nm (Figure 1). This startling observation became easily comprehensible if one considered the structure, which was much-more-rigidly twisted than in compound **2** (computational results indicated an almost-orthogonal orientation of the two PBI π-systems; Figure 2). In contrast to compound **2**, the broadening was reduced because the structure of compound **9** was forced to be rigidly twisted by the presence of the double link.

Moreover, the fluorescence spectrum of compound **9** was not substantially shifted from that of compound **1** and the fluorescence quantum yield was the highest among all of the linked diPBIs considered ($\phi_{fl}=0.44$). Triply-linked PBI (**10**) behaved significantly different to compounds **2**, **3**, and **9**. It featured the longest absorbance maximum (684 nm),[17a] which was bathochromically shifted by about 4350 cm^{-1} relative to that of compound **1**, and showed pronounced vibronic progressions. These properties could hardly be explained by excitonic interactions and were due to extensive conjugation over the whole π-system of compound **10**. These data were also supported by the MO coefficients of the HOMO−1 and the LUMO, which included the three C–C single bonds that connected the two PBIs to form a rigid, almost-planar "step ladder" superstructure (Figure 2). The fluorescence spectra showed a small Stokes shift (170 cm^{-1}) but an almost negligible quantum yield ($\phi_{fl}=0.02$).

Electrochemistry: The CVs were measured in CH_2Cl_2 with Bu_4NPF_6 (0.1 M) as the electrolyte and were referenced against the Fc/Fc^+ redox couple (Table 1). The CVs of compounds **2**, **9**, and **10** showed four well-defined, single-electron reversible reduction waves (Figure 3). Differential pulse voltammetry experiments showed that each wave corresponded to the transfer of a single electron (see the Supporting Information, Figure S4). Compared with PBI, the half-wave reduction potentials versus Fc/Fc^+ were −0.83, −0.98, −1.14, and −1.25 V for compound **2**, −0.80, −0.96, −1.07, and −1.22 V for compound **9**, and −0.46, −0.73,

Table 1. Optical and electrochemical properties of bay-linked oligo-PBIs versus PBI (**1**).

Compound	λ_{max}^{abs} [nm][a]	ε [$M^{-1}cm^{-1}$][a]	λ_{onset}^{abs} [nm][a]	λ_{max}^{fluo} [nm][a]	ϕ_{fl}[b]	E_{1r}[c]	E_{2r}[c]	E_{3r}[c]	E_{4r}[c]	E_{LUMO}[d]	E_g[e]
1	527	80900	540	534	1.00	−0.96	−1.22	–	–	−3.91	2.30
2	533	66200	590	605	0.15	−0.83	−0.98	−1.14	−1.25	−4.04	2.09
3	537	108500	620	632	0.26	−0.76	−0.96	−1.12	–	−4.11	2.01
9	531	91600	550	552	0.44	−0.80	−0.96	−1.07	−1.22	−4.07	2.25
10	684	87000	705	692	0.02	−0.46	−0.73	−1.49	−1.66	−4.36	1.85

[a] Measured in dilute $CHCl_3$ (1.0×10^{-5} M); [b] average deviation for ϕ_{fl} (±0.04) was determined by using compound **1** (*N*,*N*′-di(2,6-diisopropylphenyl)-perylene-3,4:9,10-tetracarboxylic acid bisimide, $\phi_{fl}=1.00$ in $CHCl_3$) as the standard; [c] half-wave potential in CH_2Cl_2 versus Fc/Fc^+; [d] LUMO estimated by the onset of the reduction peaks and calculated according to $E_{LUMO}=-(4.8+E_{onset})$; [e] calculated by the onset of absorption in $CHCl_3$ according to $E_g=1240/\lambda_{onset}$.

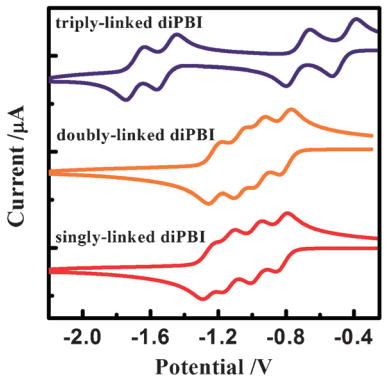

Figure 3. Reductive CVs of compounds **2** (red), **9** (orange), and **10** (violet) in CH_2Cl_2 (electrolyte: 0.1 M Bu_4NPF_6; scan rate: 100 mV s^{-1}; versus Fc/Fc^+).

−1.49, and −1.66 V for compound **10**, thereby indicating the much-higher electron-affinity of triply-linked diPBI as a reflection of the electronic coupling between the adjacent PBI units. Compounds **2** and **9** displayed much-smaller shifts, which further supported the electronic decoupling of these non-conjugated oligo-PBIs. The LUMO levels, which were estimated from the onset of reduction potentials, were −4.04 eV for compound **2**, −4.07 eV for compound **9**, and −4.36 eV for compound **10**, which was significantly smaller (nearly 0.3 eV) than the highly twisted diPBIs (**2** and **9**).

Spectroelectrochemistry: To gain further insight into the electronic structure of the charges in compounds **2**, **9**, and **10**, we performed UV/Vis/NIR spectroelectrochemical experiments in CH_2Cl_2/Bu_4NPF_6 (0.2 M). Thus, specific electrical potentials were applied to a polished platinum disk electrode and UV/Vis/NIR spectra were recorded. Owing to the relatively large redox-potential separations between the four redox processes for each compound, there were potentials at which a specific radical ion could almost exclusively be generated (in all cases, more than 80% of all molecules). Thus, the recorded spectra at these potentials were taken as those of the "pure" radical ion without further deconvolution. These spectra are shown in Figure 4 versus the wavenumbers for a better comparison with the computed spectra.

First inspection of the spectroelectrochemistry of compounds **2** and **9** revealed very similar behavior up to the spectra of the tetra-anion, which was due to their twisted structures. For both compounds, reduction into the radical mono-anion resulted in a decrease of the lowest-energy transition at about 20000 cm^{-1} to roughly 50% of its original intensity (if one takes the integral of the band), whilst new transitions appeared between 10000 and 17000 cm^{-1}. Upon reduction to the radical di-anion, the band at 20000 cm^{-1} disappeared almost completely whilst that between 10000 and 17000 cm^{-1} doubled in intensity. Further reduction to the tri-anion again led to an approximate 50% decrease in intensity of the band at 10000–17000 cm^{-1} and to the appearance of a new band in the range 14000–22000 cm^{-1}. This latter band doubled on reduction to the tetra-anion, whilst the band at 10000–17000 cm^{-1} vanished. These observations suggested the presence of practically noninteracting PBI units in compounds **2** and **9**, whose spectroscopic properties were additive. In other words, any charge that was added to compound **2** or compound **9** was completely localized on either of the two PBI units. However, in particular for the di-anion of compound **2** but also visible in compound **9**, a weak transition at even-lower energy than those mentioned above appeared at about 5000 cm^{-1}, which was too near to the accessible spectroscopic window of the solvent to be completely visible. A similar band, although much-less intense, was also visible at the same energy as the mono-anions and tri-anions of compounds **2** and **9**. These bands resulted from the interaction of the two PBI units and were charge-transfer bands in nature (see below). Those CT bands in the mono-anions and tri-anions of compounds **2** and **9** were so-called intervalence charge-transfer (IV-CT) bands, which are typical of MV class II compounds. Unfortunately, these bands were very weak and their maxima were beyond the accessible spectroscopic window. Thus, we were unable to evaluate the electronic couplings from these IV-CT bands by, for example, Mulliken–Hush theory.[22]

In contrast to compounds **2** and **9**, diPBI **10** showed different spectra for each redox state, which could not be reconstructed from independent units. For the mono-anion, a highly structured band in the range 6000–11000 cm^{-1} appeared that was replaced by a much-more-intense and sharp band between 7500 and 11000 cm^{-1} for the di-anion. Again, the tri-anion showed bands down to 5000 cm^{-1} that disappear upon reduction into the tetra-anion, which itself had a series of new bands at 10000 cm^{-1} and higher energy. This behavior clearly showed that, in the triply linked and rigid diPBI **10**, the charges that were introduced by stepwise reduction interacted strongly, thus confirming the delocalization of these charges over the whole diPBI.

However, a detailed experimental analysis of the spectra was difficult because the number of states involved and their electronic origin was unknown. Furthermore, the spin multiplicity of each redox state (e.g., singlet versus triplet for the di-anion, doublet versus quartet for the tri-anion, and singlet, triplet, or quintet for the tetra-anion) was unknown but may result in distinguishable absorption spectra that could be used to compare the theoretical and experimental data to allow for unequivocal peak assignment. Thus, we performed quantum-chemical calculations at the DFT level to address these questions.

Computational results: As mentioned above, our structure-optimizations afforded a twisted structure for diPBI **2**, an almost-orthogonal structure for compound **9**, and an almost-planar structure for compound **10**. The striking observation of an even-stronger twist in compound **9** showed that multiple linkages could induce a stronger twist because of more structural strain.

The different degrees of electronic communication in singly linked, doubly linked, and triply linked diPBIs could

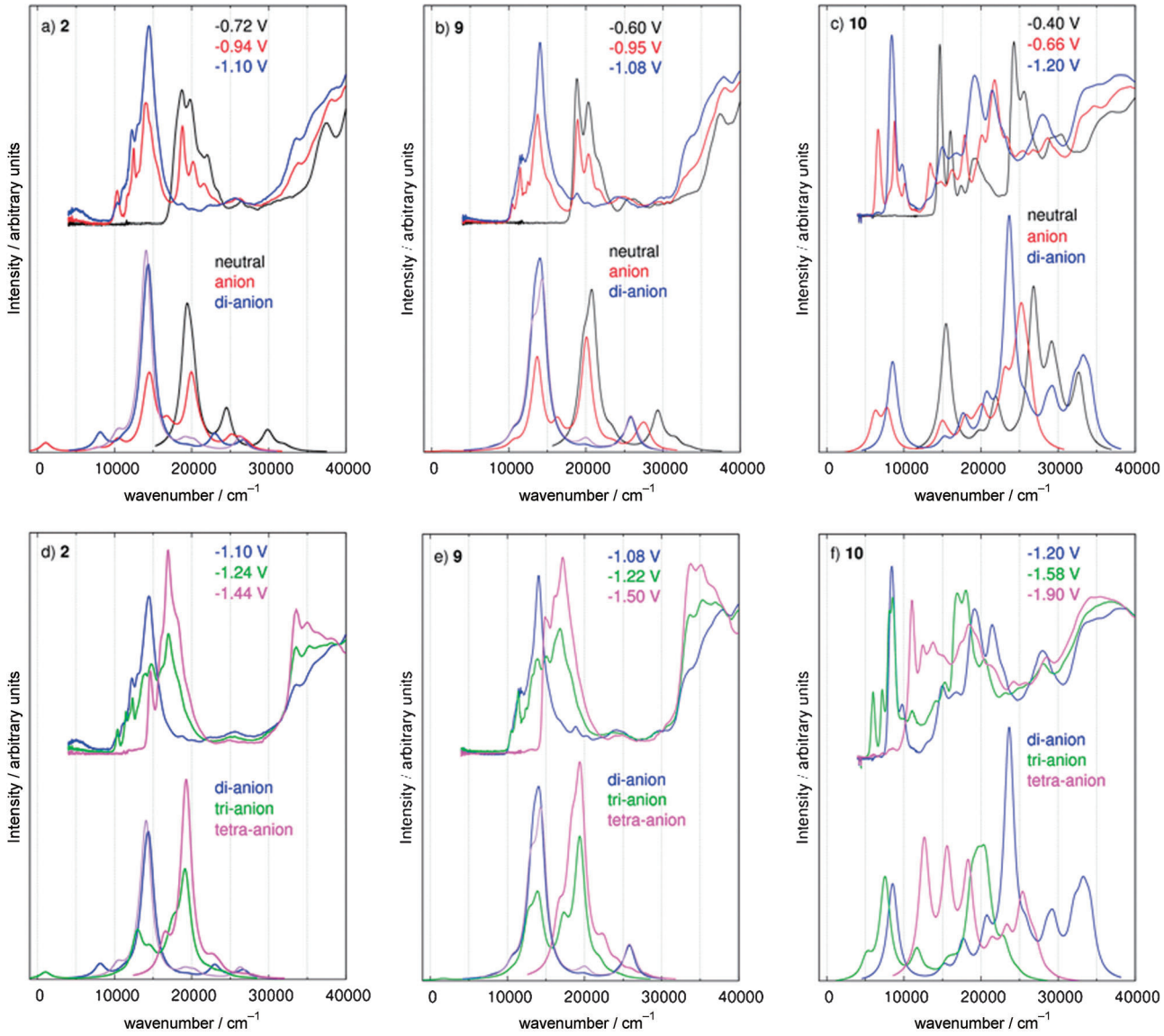

Figure 4. Comparison between the observed and computed electronic spectra of compounds **2** (a, d); **9** (b, e); and **10** (c, f). Top: CH_2Cl_2/Bu_4NPF_6 (0.2 M), versus Fc/Fc^+. Bottom: TD-CAM-B3LYP/6-31G*-computed spectra were red-shifted by 2500 cm^{-1}.

be quantified by considering the energy splitting between the LUMO and LUMO+1 orbitals of the neutral species (for the optimized molecular structures, see Figure 2 and Figure 5).[23] Such splitting, which corresponded to twice the electronic coupling (V) according to the energy-splitting-in-dimer (ESD) method combined with Koopmans' Theory (KT),[24] was 7813 cm^{-1} (CAM-B3LYP/6-31G*) for compound **10**. Thus, the electronic coupling between the two PBI chromophores was 3900 cm^{-1}, which should be compared with the intramolecular reorganization energy (λ_i) that was associated with the PBI-anion formation (about 0.28 eV or 2300 cm^{-1} in the gas phase).[25] Therefore, triply linked diPBIs were expected to be Robin–Day class III systems in the gas phase and in nonpolar solvents, such as CH_2Cl_2.

For doubly linked and singly linked diPBIs, the situation was more critical because the electronic coupling diminished to 809 cm^{-1} for the singly linked diPBI and to 255 cm^{-1} for the doubly linked diPBI, thus indicating that these systems should localize the charge on a single PBI unit (Robin–Day class II) rather than allowing full delocalization.

Single-electron localization was predicted for both the mono- and tri-anionic forms of the singly- and doubly linked diPBIs, which was in accordance with their modest electronic couplings compared to compound **10**. The bond lengths for compound **9**, which showed the charge-localization, are given in Figure 6. Symmetry-breaking of the atomic structure of the mono-anion (red), which indicated localization of the electron on a single PBI unit, was clearly evident by comparison with the bond lengths of the neutral (black) and di-anion structures (blue). Similarly, for the tri-anion, the

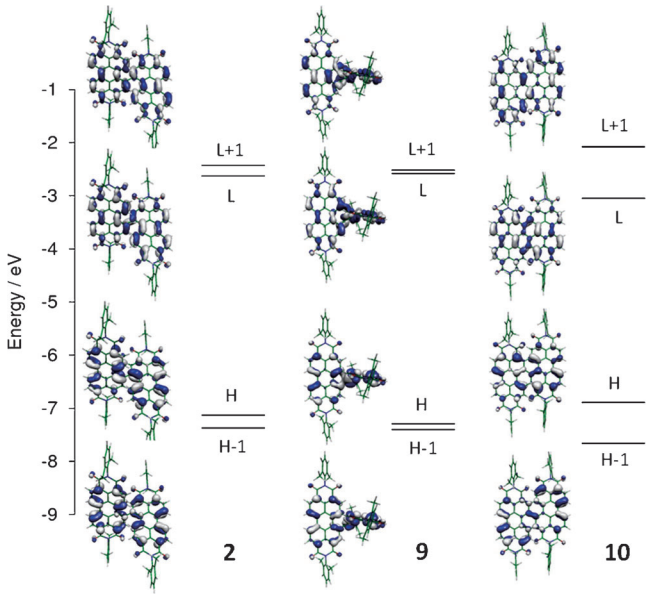

Figure 5. CAM-B3LYP/6-31G* frontier molecular orbitals of neutral compounds **2**, **9**, and **10**; the larger electronic communication in compound **10** compared to compounds **2** and **9** resulted in a large energy split in the LUMO/LUMO+1 and HOMO/HOMO−1 pairs of orbitals.

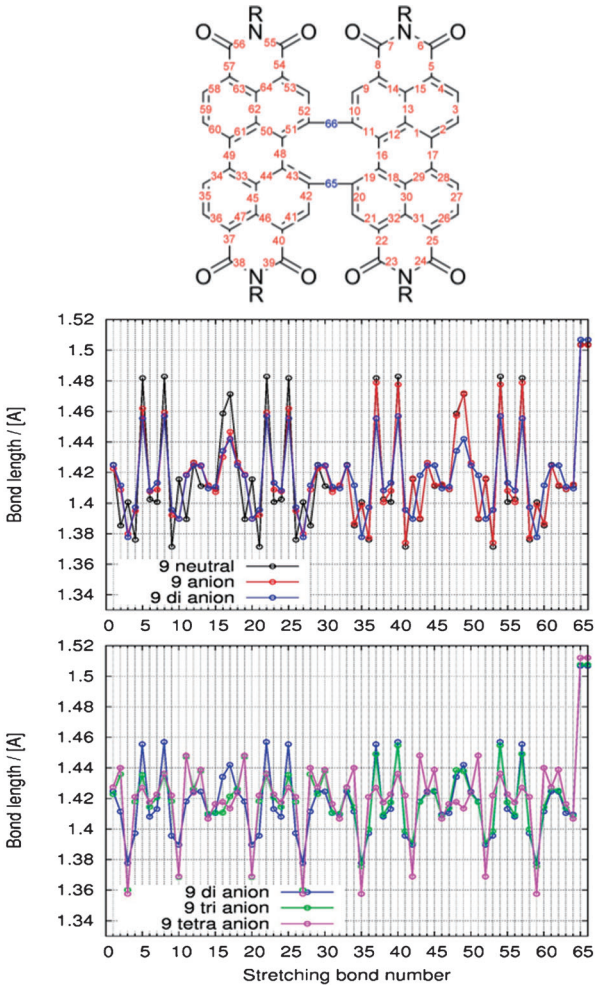

Figure 6. CAM-B3LYP/6-31G* equilibrium bond-lengths for the neutral and anionic species of compound **9**.

bond lengths indicated localization of one electron on one PBI unit and of two electrons on the other PBI unit. Similar results were obtained for compound **2** (see the Supporting Information, Figure S5), whilst a gradual change in geometry with delocalization over the two PBI units was predicted for the triply linked diPBI (see the Supporting Information, Figure S6).

The small electronic communication between the PBI units in compounds **2** and **9**, which was responsible for charge-localization in the mono- and tri-anions, also implied a biradical character of the di-anions. To determine the role of the biradicaloid contributions in the di-anion (and tetra-anion) forms of compounds **2**, **9**, and **10**, the stability of the CAM-B3LYP/6-31G* closed shell (CS) wavefunction was determined at the optimized geometry. Instability was only found for compounds **2** and **9** in their di-anionic forms, whose UCAM-B3LYP broken symmetry (BS) equilibrium geometry was determined and used to compute the electronic absorption spectra. The BS stable structures of compounds **2** and **9** were more-stable than the CS structures by 10.21 and 11.67 kcal mol^{-1}, respectively, and were almost degenerate with the triplet state (see the Supporting Information, Table S1). A comparison of the computed bond lengths for the singlet CS and BS structures, along with the triplet states, is given in the Supporting Information, Figures S7–S9.

Whilst for the di-anions of compounds **2** and **9**, the triplet and singlet states were predicted to be very close in energy, the triplet state of the di-anion of compound **10** was 11.86 kcal mol^{-1} (0.51 eV) above the singlet state; therefore, we safely concluded that the di-anion was its singlet state. Apart from the di-anionic species, the lowest-energy spin state of the other anionic forms was confirmed to be a singlet state (for tetra-anions) and a doublet for the tri-anions, with higher spin states being typically more than 1.0 eV above the lowest-energy state (see the Supporting Information, Table S1). Therefore, electronic absorption spectra were computed for the most-stable spin state of all of the species considered except for the di-anion for which the spectrum of the triplet state was also evaluated for compounds **2** and **9** (Figure 4).

Figure 4 shows a remarkable agreement between the computed and observed spectra, which suggested that the optimized atomic structures and, more specifically, the localization versus delocalization pattern (provided by CAM-B3LYP calculations) was not only consistent with the computed magnitude of the electronic couplings (see above), but also with the electronic absorption features that were observed in the spectroelectrochemical investigation.

The finer details of the computed spectra can be found in the Supporting Information, Figures S10–S12. Reduction to the mono-anions of compounds **2** and **9** resulted in a decrease in the intensity of the band at 20000 cm^{-1} and the ac-

companying appearance of a number of new electronic transitions (see the Supporting Information, Figures S10 and S11) in the 15000 cm^{-1} region, which was in agreement with the experimental results. Upon further reduction, the appearance and disappearance of the electronic transitions was closely reproduced by the calculations. The correlation between the computed and observed data confirmed the similarity of the spectroscopic signatures of compounds **2** and **9** with the charge-localization that was induced by their decreased electronic communication.

The spectra of the di-anionic forms of compounds **2** and **9** deserved an additional comment: for each species, both the computed spectrum for the triplet state and the computed spectrum for the BS singlet state (Figure 4). These two spectra were very similar, on account of the similar predicted geometries for BS singlet and triplet states. Nevertheless, for the singlet state, a weak feature that was not computed for the triplet state was found at about 7500 cm^{-1}. This feature was clearly visible as a weak isolated band in the spectrum of compound **2**, whilst it was just a shoulder in the spectrum of compound **9**. This band had the same origin for both compounds and was due to a charge-transfer (CT) excitation from the localized molecular orbitals, as shown in Figure 7a for the singly-linked compound. In this respect, the term "charge transfer" might be somewhat misleading because in total, no charge was transferred and there was no change in the dipole moment upon excitation. However, the individual MO contributions of the excitations were clearly CT in nature, which prompted us to call this type of excitation "quasi-CT". Interestingly, the experimental spectra of the di-anion showed a feature at 5000 cm^{-1}, which was slightly more intense for compound **2** than for compound **9** and which could be attributed to the CT transition. Therefore, even considering possible inaccuracies in the description of BS singlet states owing to spin contamination, based on the comparison between computed and experimental spectra, we concluded that only the singlet state of the di-anions of compounds **2** and **9** accounted for the weak CT band that was observed in the spectroelectrochemical study.

A similar weak feature, which was shifted to even-lower energy (about 1000 cm^{-1}) was computed for the mono- and tri-anionic forms of compounds **2** and **9**; this feature was due to an IV-CT excitation, as shown in Figure 7b for the singly linked diPBI. Indeed, the experimental counterpart of the computed CT band was observed in the low-energy portion of the spectra (Figure 4). The analogy of MO excitations in the mono- and tri-anions of compound **2** (Figure 7b) also supported our assignment of the low-energy band of the di-anion (Figure 7a) as a CT excitation.

The electronic transitions of compound **10** were determined by the strong electron interaction between the two PBI units; therefore, they were remarkably different from those of compounds **2** and **9**. The close agreement between the computed and observed spectra suggested that the degree of electronic coupling in compound **10** was also realistically accounted for by the CAM-B3LYP calculations.

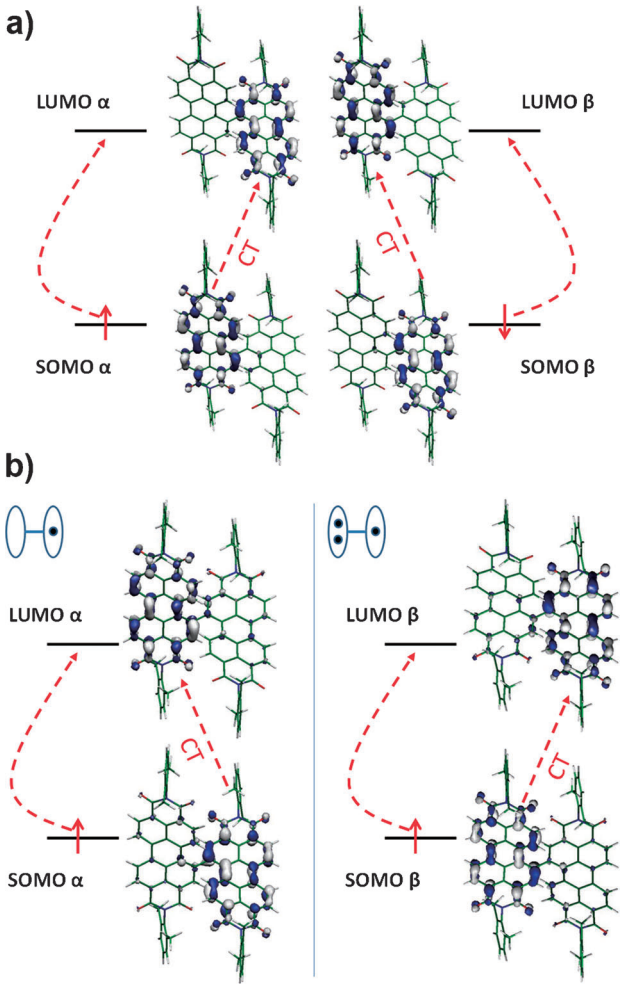

Figure 7. a) The localized nature of the UCAM-B3LYP/6-31G* SOMO and LUMO (α and β) orbitals in the BS biradical structure of the di-anion of compound **2**. The two electronic excitations that were responsible for the low-energy (computed value: 7500 cm^{-1}, observed value: 5000 cm^{-1}) quasi-CT transition are indicated by dashed red arrows. b) The localized nature of the SOMO and LUMO (α) orbitals of the mono-anion of compound **2** (left) and the SOMO and LUMO (β) orbitals of the tri-anion of compound **2** (right). These orbitals were involved in the electronic excitation that was responsible for the low-energy (computed value: about 1000 cm^{-1}) CT transition, as indicated by the dashed red arrow. A schematic representation of the electron localization on the singly linked diPBI, as determined by UCAM-B3LYP/6-31G* calculations, is shown in the top-left corner of each graph.

Conclusion

We used the copper-mediated Ullmann coupling of 1,7-dibromoperylene bisimides to construct structurally perfect singly-linked perylene-bisimide arrays along the bay regions, whilst the homo-coupling of 1,12-dibromoperylene bisimides afforded doubly linked and triply linked diperylene bisimides. Three bay-linked diperylene bisimides that differed in their linkage (singly, doubly, and triply linked) were used to investigate the PBI interactions in their neutral and reduced forms. Quantum-chemical calculations at the DFT and TDDFT levels were used to assist the interpretation of

experimental results. UV/Vis absorption and fluorescence spectroscopy revealed different degrees of interaction, which may be understood in terms of exciton coupling and conjugation effects, with the latter effect dominating the interactions in the triply linked compound (**10**). The electrochemical properties (cyclic voltammetry) as well as spectroelectrochemical analysis showed quite-different degrees of PBI interactions in the reduced molecules. Again, the singly- and doubly linked diPBIs were electronically almost decoupled but showed weak IV-CT excitations in the NIR, which resulted from weak interactions between the two PBI moieties of the mono- and tri-anions of compounds **2** and **9**, respectively. In this regard, the observation of such a quasi-CT band in the di-anions of compounds **2** and **9** was surprising in view of their symmetry, but it was explained by a mixture of two CT excitations of the α and β electrons. However, the anions of compound **10** showed excitations that were due to the delocalized wavefunction of the π-system. In contrast to our initial expectations, the degree of interaction in both the neutral and the reduced forms of the bay-linked PBIs did not follow the order of the number of linkers but rather qualitatively followed the order: doubly linked < singly linked ≪ triply linked, owing to the different degrees of twisting between the two PBIs moieties.

Experimental Section

Materials and methods: All chemicals and solvents were purchased from commercial suppliers and used without further purification unless otherwise specified. DMSO was freshly distilled from CaH_2. *N,N′*-di(2,6-diisopropylphenyl)perylene-3,4:9,10-tetracarboxylic acid bisimide (PBI, **1**) and *N,N′*-di(2,6-diisopropylphenyl)-1,6,7,12-tetrabromoperylene-3,4:9,10-tetracarboxylic acid bisimide (**7**) were synthesized according to literature procedures.[26] 1-Bromoperylene bisimide (**5**) and 1,7-dibromoperylene bisimide (**6**) were prepared according to our previously reported procedure.[18]

^{1}H (400 MHz) and ^{13}C NMR spectra (100 MHz) were recorded on a Bruker ADVANCE 400 NMR Spectrometer. *J* values are expressed in Hz and chemical shifts (in ppm) are given downfield of tetramethylsilane (TMS) with the residual protonated solvent used as an internal standard. The signals were designated as follows: s (singlet), d (doublet), t (triplet), q (quartet), dd (doublet of doublets), and m (multiplet). MS (MALDI-TOF) were determined on a Bruker BIFLEX III Mass Spectrometer. Elemental analysis was performed on a FLASH EA1112 elemental analyzer. UV/Vis spectra were measured with a Hitachi (Model U-3010) UV/Vis spectrophotometer in a 1 cm quartz cell. Fluorescence excitation and emission spectra were recorded with a Hitachi FP-6600 FL fluorimeter at room temperature. Fluorescence quantum yields were determined by optical dilute method with *N,N′*-di(2,6-diisopropylphenyl)perylene-3,4:9,10-tetracarboxylic acid bisimide (PBI) in $CHCl_3$ as a reference ($\phi_{fl}=1.0$).[20] Cyclic voltammograms (CVs) were recorded on a Zahner IM6e electrochemical workstation at a scan rate of 100 mV s^{-1}, with glassy carbon discs as the working electrode, Pt wire as the counter electrode, Ag/AgCl electrode as the reference electrode, and ferrocene/ferrocenium as an internal potential marker for the calibration of potential. 0.1 M Bu_4NPF_6 in CH_2Cl_2 (HPLC grade) was used as the supporting electrolyte.

Spectroelectrochemistry experiments were performed in a cylindrical quartz cell with a three-electrode setup that consisted of a platinum disc working electrode (6 mm diameter), a gold-coated metal plate as counter electrode, and a Ag/AgCl pseudo-reference electrode. Measurements were performed under an argon atmosphere in a CH_2Cl_2/Bu_4NPF_6 (0.2 M) solution. The potentials were applied in 20 mV steps by using an EG&G Princeton Applied Research Model 283 potentiostat. UV/Vis/NIR spectra were recorded with a JASCO V-570 spectrophotometer in reflection mode at the polished working electrode, which was adjusted to 100 μm above the cell bottom by using a micrometer screw.

Synthesis of singly-linked diPBI (2): A Schlenk flash was charged with 1-bromoperylene bisimide (**5**, 100 mg, 0.13 mmol), copper powder (Aldrich, particle size < 100 nm, 99.8%, 81 mg, 1.27 mmol), and dry DMSO (20 mL) under an argon atmosphere. The mixture was heated at 60 °C with vigorous stirring for 8 h. Next, the cooled mixture was poured into water and extracted with CH_2Cl_2. The organic layers were separated, washed with brine, dried over Na_2SO_4, and purified by column chromatography on silica gel (petroleum ether/CH_2Cl_2, 1:2 v/v) to afford compound **2** as an red–violet solid (76 mg, 84.4%). ^{1}H NMR (400 MHz, $CDCl_3$, TMS) δ = 8.86–8.91 (m, 8H), 8.72 (d, ^3J(H,H) = 8.0 Hz, 2H), 8.33–8.35 (m, 4H), 7.45–7.50 (m, 4H; phenyl H), 7.30–7.35 (m, 8H; phenyl H), 2.64–2.82 (m, 8H; isopropyl H), 1.15–1.20 (m, 24H; isopropyl H), 1.06–1.10 ppm (m, 24H; isopropyl H); ^{13}C NMR (100 MHz, $CDCl_3$, TMS): δ = 163.69, 163.59, 163.49, 163.36, 146.11, 146.05, 145.83, 142.27, 135.63, 135.42, 135.03, 134.87, 133.83, 132.65, 131.66, 130.60, 130.51, 130.47, 130.11, 129.83, 129.40, 128.25, 127.88, 124.72, 124.55, 124.49, 124.42, 124.21, 124.14, 124.01, 123.67, 31.93, 29.51, 29.46, 24.37, 24.28, 22.99, 14.46 ppm; MS (MALDI-TOF): calcd: 1418.6 $[M]^-$; found: 1419.0; elemental analysis calcd (%) for $C_{96}H_{82}N_4O_8$: C 81.22, H 5.82, N 3.95; found: C 81.05, H 5.68, N 3.89.

Synthesis of singly-linked PBI-based oligomers: A Schlenk flash was charged with 1,7-dibromoperylene bisimide (**6**, 200 mg, 0.23 mmol), copper powder (Aldrich, particle size < 100 nm, 99.8%, 147 mg, 2.30 mmol) and dry DMSO (50 mL) under an argon atmosphere. The mixture was heated at 60 °C with vigorous stirring for 5 h. Next, the cooled mixture was poured into water and extracted with CH_2Cl_2. The organic layers were separated, washed with brine, dried over Na_2SO_4, and purified by column chromatography on silica gel (petroleum ether/CH_2Cl_2, 1:2 v/v) to afford dimer **2** (24 mg, 14.7%) and trimer **3** (16 mg, 9.8%) as red–violet solids, whilst the residual fractions contained a tetramer and other oligomers up to an octadecamer (detected by MS).

Trimer 3: ^{1}H NMR (400 MHz, [D$_6$]DMSO, TMS) δ = 9.19 (t, ^3J(H,H) = 8.0 Hz, 4H), 8.71–8.77 (m, 8H), 8.57 (s, 2H), 8.45 (s, 2H), 8.38 (t, ^3J(H,H) = 8.0 Hz, 4H), 7.21–7.44 (m, 18H; phenyl H), 2.46–2.66 (m, 12H; isopropyl H), 0.82–1.04 ppm (m, 72H; isopropyl H); ^{13}C NMR (150 MHz, $CDCl_3$, TMS): δ = 163.70, 163.56, 163.45, 163.22, 163.18, 163.13, 146.05, 146.00, 145.85, 142.77, 141.99, 135.97, 135.85, 135.06, 134.98, 134.89, 134.26, 133.48, 132.73, 132.69, 130.73, 130.60, 130.59, 130.47, 130.30, 130.12, 129.87, 129.50, 128.38, 124.75, 124.71, 124.52, 124.44, 124.34, 124.25, 124.04, 123.93, 123.73, 29.55, 29.50, 29.45, 29.43, 29.35, 24.31, 24.26 ppm; MS (MALDI-TOF): calcd: 2126.9 $[M]^-$; found: 2127.6; elemental analysis calcd (%) for $C_{144}H_{122}N_6O_{12}$: C 81.25, H 5.78, N 3.95; found: C 81.08, H 5.69, N 3.79.

1,12-Dibromoperylene bisimide (8): A mixture of tetrabromoperylene bisimide (**7**, 500 mg, 0.49 mmol), CuI (558 mg, 2.92 mmol), and L-proline (393 mg, 3.41 mmol) was heated in dry DMSO (10 mL) at 60 °C under an argon atmosphere for 24 h. Next, the cooled mixture was poured into HCl (20 mL, 1 M), and extracted with CH_2Cl_2 (3 × 50 mL). The organic layers were separated, washed with brine, dried over Na_2SO_4, and purified by column chromatography on silica gel (petroleum ether/CH_2Cl_2, 1:1 v/v) to afford compound **8** as an orange–red solid (138 mg, 32.5%, 65.1% based on the recovered 4Br-PBI). ^{1}H NMR (400 MHz, $CDCl_3$, TMS) δ = 8.94 (s, 2H), 8.84 (d, ^3J(H,H) = 8.0 Hz, 2H), 8.67 (d, ^3J(H,H) = 8.0 Hz, 2H), 7.53 (t, ^3J(H,H) = 8.0 Hz, 2H; phenyl H), 7.39 (d, ^3J(H,H) = 8.0 Hz, 4H; phenyl H), 2.73–2.82 (m, 4H; isopropyl H), 1.18–1.22 ppm (m, 24H; isopropyl H); ^{13}C NMR (100 MHz, $CDCl_3$, TMS): δ = 163.66, 162.96, 145.97, 138.02, 135.19, 133.37, 131.63, 130.54, 130.22, 130.03, 127.92, 124.63, 124.55, 124.03, 123.64, 123.22, 29.63, 29.57, 24.37 ppm; MS (MALDI-TOF): calcd: 866.1 $[M]^-$; found: 866.2; elemental analysis calcd (%) for $C_{48}H_{40}Br_2N_2O_4$: C 66.37, H 4.64, N 3.22; found: C 66.25, H 4.58, N 3.21.

Doubly linked diPBI (9): A Schlenk flash was charged with 1,12-dibromoperylene bisimide (**8**, 200 mg, 0.23 mmol), copper powder (Aldrich, particle size < 100 nm, 99.8%, 147 mg, 2.30 mmol) and dry DMSO (20 mL) under an argon atmosphere. The mixture was heated at 60°C with vigorous stirring for 12 h. Next, the cooled mixture was poured into water and extracted with CH_2Cl_2. The organic layers were separated, washed with brine, dried over Na_2SO_4, and purified by column chromatography on silica gel (petroleum ether/CH_2Cl_2, 1:2 v/v) to afford compound **9** as an orange–red solid (112 mg, 68.7%). Compound **10** was also obtained from the crude mixture as a violet solid (15 mg, 9.2%).

Compound 9: ^{1}H NMR (400 MHz, $CDCl_3$, TMS) $\delta = 8.92$ (d, $^3J(H,H) = 8.0$ Hz, 4H), 8.83 (d, $^3J(H,H) = 8.0$ Hz, 4H), 8.03 (s, 4H), 7.48 (t, $^3J(H,H) = 8.0$ Hz, 4H; phenyl H), 7.36 (d, $^3J(H,H) = 8.0$ Hz, 4H; phenyl H), 7.29 (t, $^3J(H,H) = 10.0$ Hz, 4H; phenyl H), 2.83–2.90 (m, 4H; isopropyl H), 2.61–2.68 (m, 4H; isopropyl H), 1.22 (d, $^3J(H,H) = 8.0$ Hz, 24H; isopropyl H), 1.13 (d, $^3J(H,H) = 8.0$ Hz, 12H; isopropyl H), 1.03 ppm (d, $^3J(H,H) = 8.0$ Hz, 12H; isopropyl H); ^{13}C NMR (100 MHz, $CDCl_3$, TMS): $\delta = 163.82$, 163.67, 146.37, 145.60, 140.72, 137.95, 135.47, 134.11, 132.47, 130.56, 130.19, 128.94, 127.39, 124.61, 124.50, 124.44, 123.73, 123.18, 29.50, 24.56, 24.40, 24.34, 24.21 ppm; MS (MALDI-TOF): calcd: 1416.6 $[M]^-$; found: 1416.9; elemental analysis calcd (%) for $C_{96}H_{80}N_4O_8$: C 81.33, H 5.69, N 3.95; found: C 81.25, H 5.67, N 3.92.

Computational details: Model structures for the bay-linked PBIs, which featured methyl substituents instead of isopropyl units on the phenyl rings, were optimized with density functional theory (DFT) calculations by using the CAM-B3LYP long-range-corrected functional[27] and the 6–31G* basis set. Because the problem of poor asymptotics of the xc potential is thought to be a consequence of the self-interaction energy error, which is in turn responsible for the over-delocalization, CAM-B3LYP was expected to also provide a more-realistic description of the localization of charge in our systems than the B3LYP functional. Note that the B3LYP functional predicts fully delocalized structures for all of these systems and localization was not recovered by the inclusion of solvent effects with the polarizable continuum model (PCM) approach.[28]

The tendency of CAM-B3LYP to overestimate the excitation energy (in particular for valence excitations)[29] is well-known and, therefore, all of the computed spectra were rigidly red-shifted by 2500 cm^{-1}. Moreover, CAM-B3LYP was recently shown to be preferable to other functionals, and in particular to B3LYP, for TD-DFT calculations of excitation energies and properties, especially those that involve charge-transfer (CT) states, because it can give a balanced description of local, Rydberg, and CT excitations.[30] CAM-B3LYP was also recently used to simulate the CD spectra of doubly linked diPBIs.[16]

From a computational point of view, the correct description of a biradical contribution requires one to go beyond the single determinant approximation, whose limit is readily established by checking the stability of the wavefunction. An alternative to the computationally expensive multi-determinant approaches is to relax the constraint of identical spatial occupation for the α and β electrons, as in the unrestricted approach. Spin-restricted closed-shell (CS) calculations for the singlet states were performed with the CAM-B3LYP functional. The stability of the singlet state CS wavefunction was tested for each compound (the keyword stable = opt was used)[31] in the dianion and tetra-anion states; for those molecules that showed instability of the CS wavefunction, we determined the stable broken symmetry (BS) wavefunction[32] (open-shell biradicaloid configuration) and we also optimized the molecular structure at the unrestricted UCAM-B3LYP (BS) level. In addition, the lowest-energy triplet states (T1) were optimized at the UCAM-B3LYP level.

Orbital pictures were prepared with the Molekel 4.3 visual software.[33] Electronic excitation energies and oscillation strengths were computed for the thirty lowest singlet excited states of the investigated compounds with time-dependent (TD) CAM-B3LYP calculations. In plotting the computed electronic spectra, a Lorentzian linewidth of 0.2 eV was superimposed onto each computed intensity to facilitate the comparison with the experimental spectra. The computed spectra did not include the vibronic structure that was associated with electronic bands and, as a result, they show a smaller number of bands than the experimental spectra. All of the quantum-chemical calculations were performed with the Gaussian09 package.[34]

Whilst non-covalently linked aggregates of perylene bisimides needed more-elaborate methods to cover their electronic structure in the excited state,[35] our above-outlined procedure appeared to be sufficiently reliable to treat the electronic aspects of the covalently linked PBIs used herein.

Acknowledgements

For financial support of this research in China, we thank the National Natural Science Foundation of China (Grant Nos: 91027043, 21021091), the 973 Program (Grant No. 2011CB932301), NSFC–DFG joint project TRR61, and the Chinese Academy of Sciences. The research in Germany was supported by the Deutsche Forschungsgemeinschaft through the Graduiertenkolleg GRK 1221. The research in Italy was supported by PRIN Project 2008 JKBBK4 "Tracking ultrafast photoinduced intra- and inter-molecular processes in natural and artificial photosensors".

[1] a) R. E. Martin, F. Diederich, *Angew. Chem.* **1999**, *111*, 1440; *Angew. Chem. Int. Ed.* **1999**, *38*, 1350; b) M. Gross, D. C. Müller, H. G. Nothofer, U. Scherf, D. Neher, C. Brauchle, K. Meerholz, *Nature* **2000**, *405*, 661; c) J. M. Tour, *Chem. Rev.* **1996**, *96*, 537; d) T. Dutta, K. B. Woody, S. R. Parkin, M. D. Watson, J. Gierschner, *J. Am. Chem. Soc.* **2009**, *131*, 17321; e) A. Tsuda, A. Osuka, *Science* **2001**, *293*, 79; f) M. Baumgarten, M. Müller, A. Bohnen, K. Müllen, *Angew. Chem.* **1992**, *104*, 482; *Angew. Chem. Int. Ed. Engl.* **1992**, *31*, 448; g) J. Wu, M. D. Watson, N. Tchebotareva, Z. Wang, K. Müllen, *J. Org. Chem.* **2004**, *69*, 8194.

[2] a) A. Heckmann, C. Lambert, *Angew. Chem. Int. Ed.* **2012**, *51*, 326; b) J. Hankache, O. S. Wenger, *Chem. Rev.* **2011**, *111*, 5138.

[3] J. L. Brédas, D. Beljonne, V. Coropceanu, J. Cornil, *Chem. Rev.* **2004**, *104*, 4971.

[4] J. L. Brédas, G. B. Street, *Acc. Chem. Res.* **1985**, *18*, 309.

[5] M. B. Robin, P. Day, *Adv. Inorg. Chem. Radiochem.* **1967**, *9*, 247.

[6] a) B. S. Brunschwig, C. Creutz, *Chem. Soc. Rev.* **2002**, *31*, 168; b) S. F. Nelsen, *Chem. Eur. J.* **2000**, *6*, 581; c) K. D. Demadis, C. M. Hartshorn, T. J. Meyer, *Chem. Rev.* **2001**, *101*, 2655; d) J. P. Launay, C. Coudret, C. Hortholary, *J. Phys. Chem. B* **2007**, *111*, 6788.

[7] a) R. A. Marcus, *Pure Appl. Chem.* **1997**, *69*, 13; b) R. A. Marcus, N. Sutin, *Comments Inorg. Chem.* **1986**, *5*, 119.

[8] a) P. Chen, T. J. Meyer, *Chem. Rev.* **1998**, *98*, 1439; b) S. F. Nelsen, H. Q. Tran, *J. Phys. Chem. A* **1999**, *103*, 8139; c) B. S. Brunschwig, S. Ehrenson, N. Sutin, *J. Phys. Chem.* **1986**, *90*, 3657; d) S. F. Nelsen, D. A. Trieber, R. F. Ismagilov, Y. Teki, *J. Am. Chem. Soc.* **2001**, *123*, 5684.

[9] K. Hunger, *Industrial Dyes: Chemistry, Properties, Applications*, Wiley-VCH, Weinheim, **2003**.

[10] a) F. Würthner, *Chem. Commun.* **2004**, 1564; b) T. van der Boom, R. T. Hayer, Y. Zhao, P. J. Bushar, E. A. Weiss, M. R. Wasielewski, *J. Am. Chem. Soc.* **2002**, *124*, 9582; c) Y. Che, A. Datar, K. Balakrishnan, L. Zang, *J. Am. Chem. Soc.* **2007**, *129*, 7234; d) C. Addicott, I. Oesterling, T. Yamamoto, K. Müllen, P. J. Stang, *J. Org. Chem.* **2005**, *70*, 797; e) X. He, H. Liu, Y. Li, S. Wang, Y. Li, N. Wang, J. Xiao, X. Xu, D. Zhu, *Adv. Mater.* **2005**, *17*, 2811.

[11] a) M. P. O'Neil, M. P. Niemczyk, W. A. Svec, D. Gosztda, G. L. Gaines, M. R. Wasielewski, *Science* **1992**, *257*, 63; b) J. J. Dittmer, E. A. Marseglia, R. H. Friend, *Adv. Mater.* **2000**, *12*, 1270; c) B. A. Jones, M. J. Ahrens, M. Yoon, A. Facchetti, T. J. Marks, M. R. Wasielewski, *Angew. Chem.* **2004**, *116*, 6523; *Angew. Chem. Int. Ed.* **2004**, *43*, 6363; d) B. A. Jones, A. Facchetti, M. R. Wasielewski, T. J. Marks, *J. Am. Chem. Soc.* **2007**, *129*, 15259; e) Y. Che, H. Huang, M. Xu, C. Zhang, B. R. Bunes, X. Yang, L. Zang, *J. Am. Chem. Soc.* **2011**, *133*, 1087.

[12] a) X. Zhan, Z. Tan, B. Domercq, Z. An, X. Zhang, S. Barlow, Y. Li, D. Zhu, B. Kippelen, S. R. Marder, *J. Am. Chem. Soc.* **2007**, *129*,

7246; b) J. H. Oh, W. Y. Lee, T. Noe, W. C. Chen, M. Könemann, Z. Bao, *J. Am. Chem. Soc.* **2011**, *133*, 4204.
[13] a) C. Kohl, S. Becker, K. Müllen, *Chem. Commun.* **2002**, 2778; b) N. G. Pschirer, C. Kohl, F. Nolde, J. Qu, K. Müllen, *Angew. Chem.* **2006**, *118*, 1429; *Angew. Chem. Int. Ed.* **2006**, *45*, 1401.
[14] a) Q. Yan, D. Zhao, *Org. Lett.* **2009**, *11*, 3426; b) Z. Yuan, Y. Xiao, X. Qian, *Chem. Commun.* **2010**, *46*, 2772.
[15] a) J. Hassan, M. Sévignon, C. Gozzi, E. Schulz, M. Lemaire, *Chem. Rev.* **2002**, *102*, 1359; b) D. Ma, Q. Cai, *Acc. Chem. Res.* **2008**, *41*, 1450; c) S. V. Ley, A. W. Thomas, *Angew. Chem.* **2003**, *115*, 5558; *Angew. Chem. Int. Ed.* **2003**, *42*, 5400; d) I. P. Beletskaya, A. V. Cheprakov, *Coord. Chem. Rev.* **2004**, *248*, 2337; e) F. Monnier, M. Taillefer, *Angew. Chem.* **2009**, *121*, 7088; *Angew. Chem. Int. Ed.* **2009**, *48*, 6954; f) Y. Li, L. Tan, Z. Wang, H. Qian, Y. Shi, W. Hu, *Org. Lett.* **2008**, *10*, 529; g) Y. Li, C. Li, W. Yue, W. Jiang, R. Kopecek, J. Qu, Z. Wang, *Org. Lett.* **2010**, *12*, 2374.
[16] Y. Zhen, W. Yue, Y. Li, W. Jiang, S. Di Motta, E. Di Donato, F. Negri, S. Ye, Z. Wang, *Chem. Commun.* **2010**, *46*, 6078.
[17] a) H. Qian, Z. Wang, W. Yue, D. Zhu, *J. Am. Chem. Soc.* **2007**, *129*, 10664; b) Y. Shi, H. Qian, Y. Li, W. Yue, Z. Wang, *Org. Lett.* **2008**, *10*, 2337; c) H. Qian, F. Negri, C. Wang, Z. Wang, *J. Am. Chem. Soc.* **2008**, *130*, 17970; d) H. Qian, W. Yue, Y. Zhen, S. Di Motta, E. Di Donato, F. Negri, J. Qu, W. Xu, D. Zhu, Z. Wang, *J. Org. Chem.* **2009**, *74*, 6275; e) Y. Zhen, H. Qian, J. Xiang, J. Qu, Z. Wang, *Org. Lett.* **2009**, *11*, 3084; f) Y. Zhen, C. Wang, Z. Wang, *Chem. Commun.* **2010**, *46*, 1926; g) Y. Wu, Y. Zhen, Y. Ma, R. Zheng, Z. Wang, H. Fu, *J. Phys. Chem. Lett.* **2010**, *1*, 2499; h) H. Wang, H. Su, H. Qian, Z. Wang, X. Wang, A. Xia, *J. Phys. Chem. A* **2010**, *114*, 9130.
[18] W. Jiang, Y. Li, W. Yue, Y. Zhen, J. Qu, Z. Wang, *Org. Lett.* **2010**, *12*, 228.
[19] a) A. D. Schlüter, M. Löffler, V. Enkelmann, *Nature* **1994**, *368*, 831; b) C. Xu, A. Wakamiya, S. Yamaguchi, *J. Am. Chem. Soc.* **2005**, *127*, 1638; c) U. Scherf, K. Müllen, *Makromol. Chem. Rapid Commun.* **1991**, *12*, 489; d) Y. Wu, J. Zhang, Z. Fei, Z. Bo, *J. Am. Chem. Soc.* **2008**, *130*, 7192.
[20] C. You, R. Dobrawa, C. R. S. Möller, F. Würthner, *Top. Curr. Chem.* **2005**, *258*, 39.
[21] M. Kasha, H. R. Rawls, M. Ashraf El-Bayoumi, *Pure Appl. Chem.* **1965**, *11*, 371.
[22] a) N. S. Hush, *Coord. Chem. Rev.* **1985**, *64*, 135; b) N. S. Hush, *Electrochim. Acta* **1968**, *13*, 1005; c) S. F. Nelsen, R. F. Ismagilov, D. A. Trieber, *Science* **1997**, *278*, 846.
[23] F. Cisnetti, R. Ballardini, A. Credi, M. T. Gandolfi, S. Masiero, F. Negri, S. Pieraccini, G. P. Spada, *Chem. Eur. J.* **2004**, *10*, 2011.
[24] V. Coropceanu, J. Cornil, D. A. da Silva, Y. Olivier, R. Silbey, J. L. Bredas, *Chem. Rev.* **2007**, *107*, 926.
[25] a) E. Di Donato, R. P. Fornari, S. Di Motta, Y. Li, Z. Wang, F. Negri, *J. Phys. Chem. B* **2010**, *114*, 5327; b) S. Di Motta, M. Siracusa F. Negri, *J. Phys. Chem. C* **2011**, *115*, 20754.
[26] a) Y. Geerts, H. Quante, H. Platz, R. Mahrt, M. Hopmeier, A. Bohm, K. Müllen, *J. Mater. Chem.* **1998**, *8*, 2357; b) H. Quante, K. Müllen, *Angew. Chem.* **1995**, *107*, 1487; *Angew. Chem. Int. Ed. Engl.* **1995**, *34*, 1323; c) L. Fan, Y. Xu, H. Tian, *Tetrahedron Lett.* **2005**, *46*, 4443; d) W. Qiu, S. Chen, X. Sun, Y. Liu, D. Zhu, *Org. Lett.* **2006**, *8*, 867.
[27] T. Yanai, D. P. Tew, N. C. Handy, *Chem. Phys. Lett.* **2004**, *393*, 51.
[28] a) M. Renz, K. Theilacker, C. Lambert, M. Kaupp, *J. Am. Chem. Soc.* **2009**, *131*, 16292; b) M. Kaupp, M. Renz, M. Parthey, M. Stolte, F. Würthner, C. Lambert, *Phys. Chem. Chem. Phys.* **2011**, *13*, 16973.
[29] a) D. Jacquemin, V. Wathelet, E. A. Perpète, C. Adamo, *J. Chem. Theory Comput.* **2009**, *5*, 2420; b) F. Santoro, V. Barone, R. Improta, *J. Comput. Chem.* **2008**, *29*, 957.
[30] M. J. G. Peach, P. Benfield, T. Helgaker, D. J. Tozer, *J. Chem. Phys.* **2008**, *128*, 044118-1-8.
[31] a) D. Fazzi, E. V. Canesi, F. Negri, C. Bertarelli, C. Castiglioni, *ChemPhysChem* **2010**, *11*, 3685; b) S. Di Motta, F. Negri, D. Fazzi, C. Castiglioni, E. V. Canesi, *J. Phys. Chem. Lett.* **2010**, *1*, 3334.
[32] a) A. Kikuchi, H. Ito, J. Abe, *J. Phys. Chem. B* **2005**, *109*, 19448; b) P. M. Lahti, A. S. Ichimura, J. A. Sanborn, *J. Phys. Chem. A* **2001**, *105*, 251.
[33] S. Portmann, H. P. Lüthi, Molekel, version 4.3, http://www.cscs.ch/molekel/, *Chimia* **2000**, *54*, 766.
[34] M. J. Frisch et al., Gaussian 09, revision A.02, Gaussian, Inc., Wallingford CT, **2009**.
[35] a) W. Liu, V. Settels, P. H. P. Harbach, A. Dreuw, R. F. Fink, B. Engels, *J. Comput. Chem.* **2011**, *32*, 1971; b) H. Zhao, J. Pfister, V. Settels, M. Renz, M. Kaupp, V. C. Dehm, F. Würthner, R. F. Fink, B. Engels, *J. Am. Chem. Soc.* **2009**, *131*, 15660.

Received: December 17, 2011
Published online: May 3, 2012

